Cryocrystallography and Microspectrophotometry of a Mutant (αD60N) Tryptophan Synthase $\alpha_2\beta_2$ Complex Reveals Allosteric Roles of αAsp60[†,‡]

Sangkee Rhee,[§] Edith Wilson Miles,[∥] Andrea Mozzarelli,[⊥] and David R. Davies*[,§]

Laboratory of Molecular Biology and Laboratory of Biochemistry and Genetics, National Institute of Diabetes and Digestive and Kidney Diseases, National Institutes of Health, Bethesda, Maryland 20892, and Institute of Biochemical Sciences, University of Parma, 43100 Parma, Italy

Received April 7, 1998; Revised Manuscript Received May 28, 1998

ABSTRACT: We have investigated the role of Asp60 of the α-subunit in allosteric communication between the tryptophan synthase α- and β-subunits. Crystallographic and microspectrophotometric studies have been carried out on a mutant (αD60N) tryptophan synthase $\alpha_2\beta_2$ complex which has no observable α-activity, but has substantial β-activity. Single-crystal polarized absorption spectra indicate that the external aldimine is the predominant L-serine intermediate and that the amount of the intermediate formed is independent of pH, monovalent cations, and allosteric effectors. The three-dimensional structure is reported for this mutant enzyme complexed with indole 3-propanol phosphate bound to the α-site and L-serine bound to the β-site (αD60N−IPP−Ser), and this structure is compared with that of the unliganded mutant enzyme (αD60N). In the complex, L-serine forms a stable external aldimine with the pyridoxal phosphate coenzyme at the active site of the β-subunit. The conformation of the unliganded mutant is almost identical to that of the wild type enzyme. However, the structure of the mutant complexed with IPP and serine exhibits ligand-induced conformational changes much smaller than those observed previously for another mutant enzyme in the presence of the same ligands (βK87T−IPP−Ser) [Rhee, S., Parris, K. D., Hyde, C. C., Ahmed, S. A., Miles, E. W., and Davies, D. R. (1997) *Biochemistry 36*, 7664−7680]. The αD60N−IPP−Ser $\alpha_2\beta_2$ complex does not undergo the following ligand-induced conformational changes: (1) the closure of the α-subunit loop 6 (residues 178−191), (2) the movement of the mobile subdomain (residues 93−189) of the β-subunit, and (3) the rotation of the α-subunit relative to the β-subunit. These observations show that αAsp60 plays important roles in the closure of loop 6 and in allosteric communication between the α- and β-subunits.

The bifunctional enzyme bacterial tryptophan synthase $\alpha_2\beta_2$ complex (EC 4.2.1.20) catalyzes the last two steps in the biosynthesis of L-tryptophan. In the α-reaction, IGP[1] is cleaved reversibly to G3P and indole at the active site of the α-subunit (Scheme 1A). In the β-reaction, indole undergoes a PLP-dependent reaction with L-serine to form L-tryptophan at the active site of the β-subunit (Scheme 1B). X-ray crystallographic studies have shown that the $\alpha_2\beta_2$ complex has an extended αββα arrangement and that a 25 Å long hydrophobic tunnel connects the active sites of the α- and β-subunits (*1*). It has been proposed that indole, the α-reaction product, diffuses to the β-subunit active site through this tunnel.

The reactions at the α- and β-sites of tryptophan synthase are controlled by allosteric interactions that are reciprocally communicated between the two sites (for reviews, see refs *2* and *3*). Solution studies suggest that these interactions switch the enzyme between an open, low-activity state and a closed, high-activity state (*4*−*12*). Recent X-ray crystallographic studies have provided direct evidence for these ligand-mediated conformational changes in both subunits and revealed details of the allosteric interactions (*13*). The results suggested that conformational changes are transmitted through the α-subunit−β-subunit interface by a number of interactions, including interactions between the α-subunit loop 2 (residues 53−62; green in Figure 1) and β-subunit helix 6 (residues 161−181; cyan in Figure 1). Consistent with these structural features, mutations of some of these interface residues resulted in significant changes in allosteric properties (*5*, *14*−*16*). To investigate the structural and functional roles of residues in the α-subunit loop 2, we here describe the three-dimensional structure of the mutant $\alpha_2\beta_2$ complex, in which αAsp60 is replaced by asparagine, with the substrate analogue IPP bound at the active site of the α-subunit and

[†] Microspectrophotometric work by A.M. was supported in part by funds of the National Research Council (97.04377.CT14 and Target Project on Biotechnology) and the Ministry of University and Scientific and Technological Research of Italy.

[‡] The coordinates of the structures have been deposited in the Brookhaven Protein Data Bank under the names 1beu for the αD60N−IPP−serine complex and 1a5a for the αD60N.

* To whom correspondence and reprint requests should be addressed: National Institutes of Health, Bldg. 5, Rm. 338, Bethesda, MD 20892-0560. Telephone: (301) 496-4295. Fax: (301) 496-0201.

[§] Laboratory of Molecular Biology, National Institute of Diabetes and Digestive and Kidney Diseases, National Institutes of Health.

[∥] Laboratory of Biochemistry and Genetics, National Institute of Digestive and Kidney Diseases, National Institutes of Health.

[⊥] University of Parma.

[1] Abbreviations: IGP, indole 3-glycerol phosphate; G3P, glyceraldehyde 3-phosphate; PLP, pyridoxal 5′-phosphate; IPP, indole 3-propanol phosphate; PEG, polyethylene glycol; rms, root-mean-square; BTP, Bis-Tris propane; Bicine, *N*,*N*-bis(2-hydroxyethyl)glycine.

S0006-2960(98)00779-X CCC: $15.00
Published on Web 07/03/1998

Scheme 1: Reactions at the Active Site of the α-Subunit (A) and β-Subunit (B) in the Tryptophan Synthase $\alpha_2\beta_2$ Complex

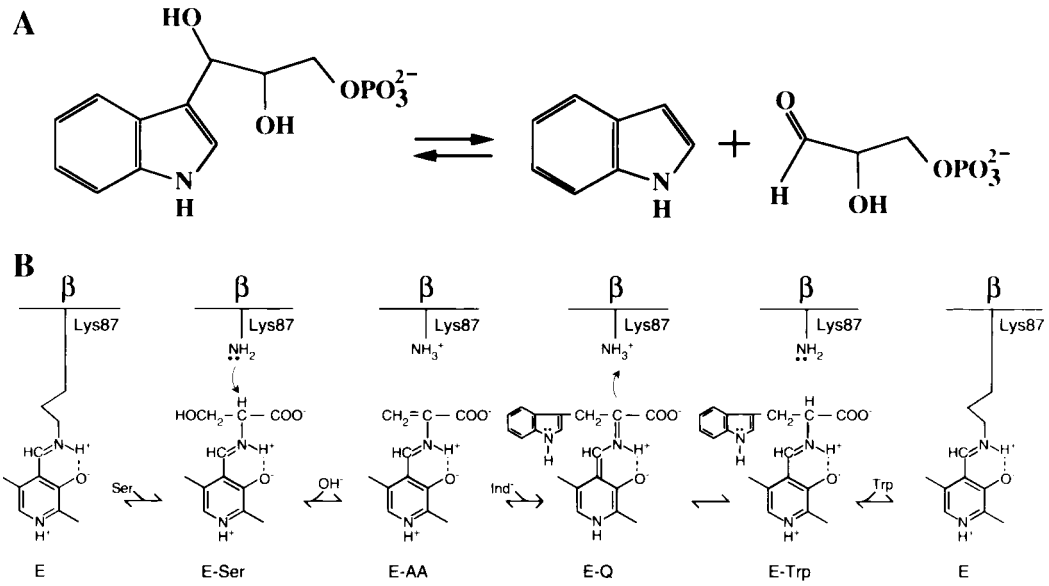

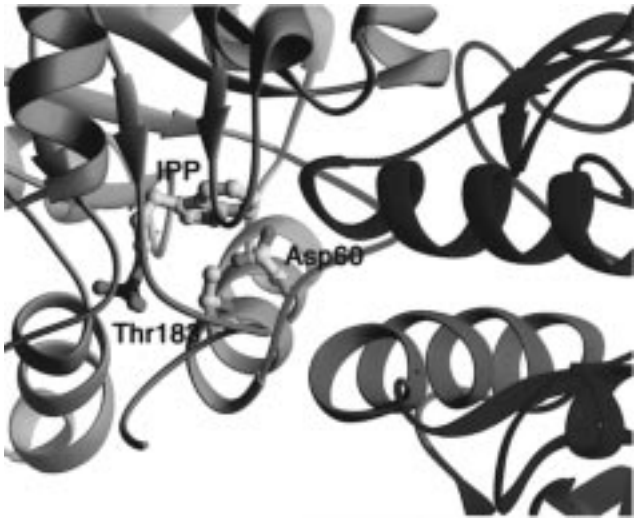

FIGURE 1: Ribbon diagram showing interactions between the α- and β-subunits where both α- and β-subunit ligands are bound to their active sites in the βK87T mutant (see ref *13*). Active site residue αAsp60 is within hydrogen-bonding distance of αThr183 and substrate analogue IPP, and these interactions seem to play key roles in enzyme reactions. Color codes are as follows: lavender for the α-subunit, green for loop 2 in the α-subunit, red for loop 6 in the α-subunit, blue for the β-subunit, and cyan for helix 6 in the β-subunit.

L-serine bound at the active site of the β-subunit (αD60N−IPP−Ser). The mutant $\alpha_2\beta_2$ complex has no measurable activity in reactions catalyzed by the α-subunit but retains substantial β-subunit activity (*17*). Microspectrophotometric studies on single crystals of this mutant enzyme have been carried out to characterize the functional properties and to define the optimal conditions for the selective accumulation of individual catalytic intermediates at the β-site.

MATERIALS AND METHODS

Crystallization and Data Collection. Mutant forms of the tryptophan synthase $\alpha_2\beta_2$ complex from *Salmonella typhimurium* were engineered and purified as described (*17*). Among several mutants at position 60 having Asp replaced with either Asn, Glu, Ala, or Tyr, only the αD60N mutant yielded crystals under the conditions used previously for crystallization of the wild type enzyme (50 mM Bicine, 1 mM Na-EDTA, 0.8−1.5 mM spermine, and 12% PEG 8000 adjusted to pH 7.8 with NaOH) (*18*). The crystals belong to a space group *C*2 with the following cell parameters: $a = 182.3$ Å, $b = 59.7$ Å, $c = 67.4$ Å, and $\beta = 94.6°$. Crystals grown in the presence of Na^+ were soaked for 1−2 days in a standard K^+-soaking solution [100 mM Bicine (pH 7.8 titrated with KOH), 1 mM EDTA, and 20% PEG 8000] (*19*), followed by soaking with the ligands, 0.1 mM IPP and 50 mM L-serine. Because L-serine bound to the β-site is slowly converted to pyruvate and ammonia by the αD60N crystals at room temperature, we have used cryocrystallography as described below.

The α-site analogue IPP was introduced by soaking the αD60N crystals in a IPP-soaking solution (0.1 mM IPP with standard K^+-soaking solution) for 1 day. The crystals were then transferred to a IPP-soaking solution having glycerol as an additional ingredient for cryoprotection. Crystals were soaked for 30 min in each concentration of glycerol (5, 10, 15, 20, and 25%) (w/v). The IPP-soaked αD60N crystals were then soaked for 15 min in 1 mL of IPP−serine-soaking solution (50 mM L-serine and 0.1 mM IPP in standard K^+-soaking solution with 30% PEG 8000) with 28% of glycerol and then were flash-frozen for data collection.

Diffraction data were collected at 95 K on an Raxis IIC imaging plate system mounted on a Rigaku RU-200 rotating anode X-ray generator operating at 50 kV and 100 mA. All diffraction data were integrated with DENZO and scaled with SCALEPACK (*20*).

Structure Determination of the αD60N−IPP−Ser $\alpha_2\beta_2$ Complex. Table 1 summarizes data statistics and refinement statistics of the complex. In the refinement of the structure with X-PLOR (*21*), the 2.0 Å wild type structure determined in the presence of K^+ at room temperature (PDB entry 1TTQ; *19*) served as a starting model. Lys87 of the β-subunit in the starting model, which forms an internal aldimine with PLP, was changed into glycine to correctly locate the bound L-serine.

Table 1: Data Collection and Refinement Statistics of the αD60N−IPP−Ser Complex

data statistics	
resolution (Å)	1.9
no. of unique reflections	49 728
average redundancy	4.5
R_{sym} (%)	5.0 (28.1)[a]
completeness (%)	87.0 (63.3)
refinement statistics	
resolution range (Å)	8.0−1.9
no. of reflections (>2σ)	45 259
average *B*-factors (Å^2)	24.0
no. of protein atoms[b]	4868
no. of solvent atoms	
water	327
cation	1 (K^+)
R_{factor}/R_{free} (%)	21.9/27.8
rms deviations from ideal	
bond length (Å)	0.007
bond angle (deg)	1.62

[a] The value in parentheses is for the last shell with a resolution of 2.0−1.9 Å. [b] Residues 177−191 in the α-subunit, substrate analogue IPP, and the coenzyme adduct between PLP and L-serine are not included.

The starting model was refined using rigid body refinement and simulated annealing refinement followed by positional and temperature factor refinements with manual rebuilding of the model using the program O (*22*) as before (*13*). In the final refined structure, L-serine forms an external aldimine with coenzyme PLP in the active site of the β-subunit, which was further confirmed by the simulated annealing omit map. Atomic models corresponding to the external aldimine and IPP were obtained from previously determined structures (*13*). Residues 178−191 in loop 6 of the α-subunit were highly disordered and could not be modeled. To evaluate effects of αD60N mutation on structure, the structure of the αD60N−IPP−Ser complex was compared with the previously determined unliganded αD60N structure (*23*).

Microspectrophotometric Measurements. Crystals of the αD60N $\alpha_2\beta_2$ complex were grown as described above. The αD60N crystals were first suspended in a solution containing 1 mM EDTA, 20% PEG 8000, 50 μM PLP, 0.08% NaN_3, either 50 mM Bicine and 250 mM NaCl or 25 mM BTP and 100 mM CsCl, at pH 7.8 and 21° C. Single-crystal polarized absorption spectra were recorded by a Zeiss MPM800 microspectrophotometer following the procedure previously described (*24*). The electric vector of the linearly polarized light was parallel to the optical axes of the *(210)* face of monoclinic *C*2 crystals.

Spectrophotometric measurements of the mutant $\alpha_2\beta_2$ complex in solution were carried out using a CARY 219 instrument interfaced to a computer for data digitalization. Enzyme solutions contained 25 mM BTP, 1 mM EDTA, and either 250 mM NaCl or 100 mM CsCl.

RESULTS

Microspectrophotometric Studies on Single Crystals of the αD60N $\alpha_2\beta_2$ Complex. We have measured the polarized absorption spectra of single crystals of the αD60N $\alpha_2\beta_2$ complex in the presence and absence of the substrate L-serine and other ligands to determine whether the crystalline enzyme forms the same enzyme−substrate intermediates at the β-site (Scheme 1B) as the soluble enzyme and whether the equilibrium distribution of these intermediates is affected by various factors.

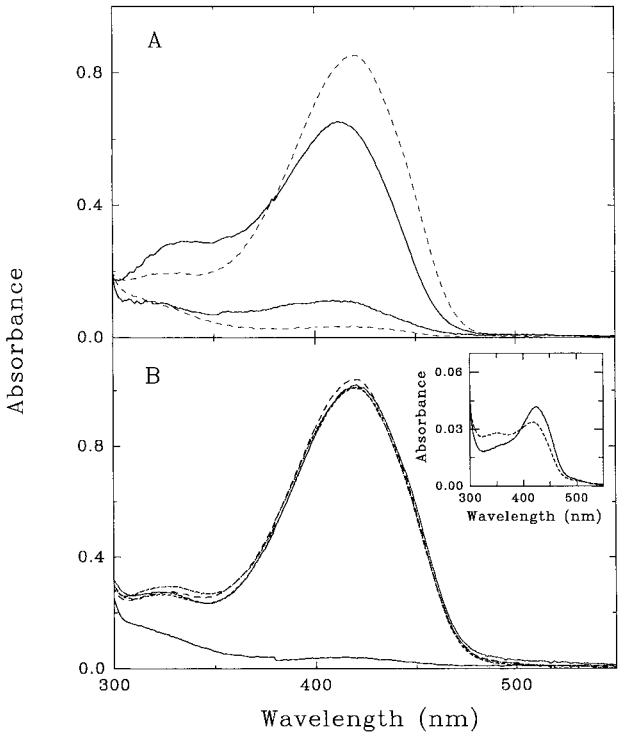

FIGURE 2: Single-crystal polarized absorption spectra of the tryptophan synthase αD60N $\alpha_2\beta_2$ complex in the presence of Na^+. A crystal of the mutant enzyme was suspended in a solution containing 50 mM Bicine, 1 mM EDTA, 20% w/v PEG 8000, and 250 mM NaCl at pH 7.8 and 21 °C. (A) Polarized absorption spectra were recorded along the *x* and *y* optical axes of the crystal (see ref *24*) in the absence (—) and in the presence of 100 mM L-serine (- -). In both cases, the higher intensity is observed along the *x* optical axis. (B) Polarized absorption spectra of the external aldimine were recorded along the *x* direction of crystals suspended in the buffer solution at pH 6.5 (—), 7.0 (-•-), 8.0 (- -), and 9.0 (••). At pH 6.5, the spectrum along the *y* axis is also shown. The inset shows the absorption spectra of a solution containing 0.5 mg/mL αD60N $\alpha_2\beta_2$ complex, 25 mM BTP, 1 mM EDTA, 250 mM NaCl, and 100 mM L-serine at pH 6 (- -) and 8.7 (—).

The polarized absorption spectrum of a single crystal of the αD60N $\alpha_2\beta_2$ complex in the absence of L-serine (Figure 2A) exhibits a peak at 412 nm and a pronounced shoulder at 340 nm, as observed for the enzyme in solution and for the wild type in the crystalline state (*24*). The reaction of L-serine with the wild type $\alpha_2\beta_2$ complex in solution leads to an equilibrium distribution of the external aldimine (E−Ser) and the α-aminoacrylate species (E−AA) (Scheme 1B). This distribution is dependent on pH and monovalent cations (*25*, *26*). Either high pH or Na^+ favors the formation of the external aldimine, whereas either low pH or Cs^+ favors the α-aminoacrylate. When a crystal of the αD60N mutant is exposed to L-serine in the presence of Na^+ (Figure 2A), the visible absorbance peak shifts to 422 nm and increases in intensity, an indication of the accumulation of the external aldimine species. The amount of the external aldimine is not affected by pH in the crystal (Figure 2B), whereas it is affected in solution (inset of Figure 2B), which is similar to the case for the wild type enzyme (*26*). When a crystal of the αD60N mutant is exposed to L-serine in the presence of Cs^+, the polarized absorption spectrum suggests that an equilibrium mixture of the external aldimine and the α-ami-

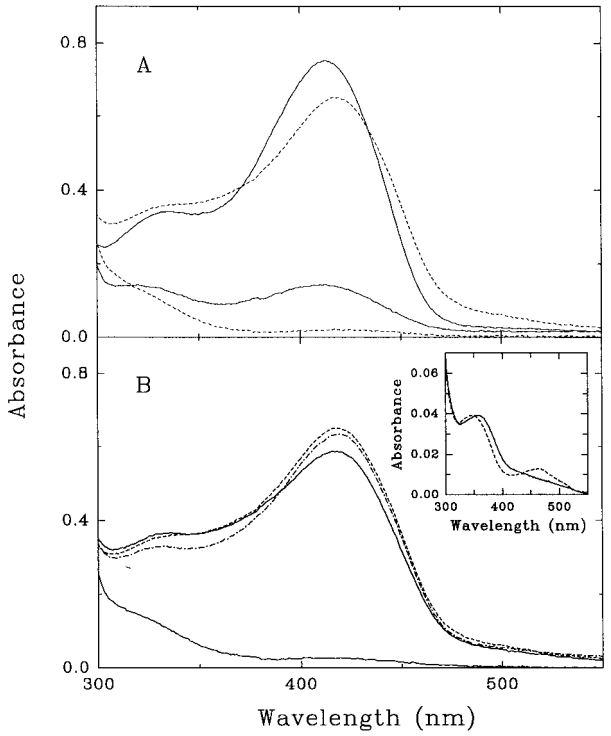

FIGURE 3: Single-crystal polarized absorption spectra of the tryptophan synthase αD60N $\alpha_2\beta_2$ complex in the presence of Cs^+. A crystal of the mutant enzyme was suspended in a solution containing 25 mM BTP, 1 mM EDTA, 20% w/v PEG 8000, and 100 mM CsCl at pH 7.9 and 21 °C. (A) Polarized absorption spectra were recorded along the *x* and *y* optical axes of the crystal (see ref *24*) in the absence (—) and in the presence of 100 mM L-serine (- -). In both cases, the higher intensity is observed along the *x* optical axis. (B) Polarized absorption spectra of the external aldimine were recorded along the *x* direction of crystals suspended in the buffer solution at pH 6.0 (—), 7.0 (- -), and 7.9 (- -). At pH 6.0, the spectrum along the *y* axis is also shown. The inset shows the absorption spectra of a solution containing 0.5 mg/mL αD60N $\alpha_2\beta_2$ complex, 25 mM BTP, 1 mM EDTA, 100 mM CsCl, and 100 mM L-serine at pH 6 (- -) and 8.7 (—).

noacrylate is present (Figure 3A). Again, the equilibrium is shifted more toward the accumulation of the external aldimine and is not significantly pH-dependent (Figure 3B). However, with the enzyme in solution, the equilibrium is displaced more toward the α-aminoacrylate (inset Figure 3B). Addition of L-serine in the presence of the α-subunit ligand glycerol 3-phosphate does not significantly affect the spectra, whereas in solution, this allosteric effector strongly favors the formation of the α-aminoacrylate for both the wild type (*26*) and the αD60N mutant (data not shown). Thus, the external aldimine of L-serine is the predominant intermediate that accumulates in crystals of the αD60N $\alpha_2\beta_2$ complex under all conditions investigated.

Crystal Structures of Bound IPP and the External Aldimine in the αD60N−IPP−Ser $\alpha_2\beta_2$ Complex. Figure 4A shows the electron density map for the bound IPP at the α-site and residues αGlu49, αAsn60, and αTyr175. The binding environment of IPP is almost identical to that in the previously determined IPP-bound structures (*13*). The product of reaction of L-serine with PLP at the β-site in the αD60N−IPP−Ser structure is shown in Figure 4B. Although the electron density for the hydroxyl group of the bound L-serine is weak relative to that of the other atoms of the coenzyme−substrate intermediate, the clear density for the tetrahedral α-carbon of L-serine (Figure 4B) indicates that the L-serine reaction product is predominantly an external aldimine (E−S in Scheme 1B), consistent with microspectrophotometric results (see above). Interactions between the external aldimine and the enzyme are shown in Figure 5. Most interactions are identical to those of other external aldimines in the βK87T mutant enzyme complexed with L-serine (*13*), with the exception of the interactions of βAsp305 and βLys87. βAsp305 interacts with the hydroxyl group of L-serine in the βK87T−Ser structure but not in the αD60N−IPP−Ser structure or in the βK87T−IPP−Ser structure. βLys87, which is proposed to catalyze the conversion from E−Ser to E−AA (Scheme 1B), is positioned perpendicular to the *si* face of the PLP ring of the external aldimine with the ϵ-amino group of βLys87 located about 4.3 Å from C_α of L-serine (see Figure 4B). A rotation of 100° around the $C_\delta-C_\epsilon$ bond of βLys87 would bring the ϵ-amino group within hydrogen-bonding distance (2.8 Å) of C_α and allow it to serve the proposed catalytic role as the acceptor of the α-proton of L-serine. The temperature factor of the ϵ-amino group (40 $Å^2$) is greater than those of the rest of the side chain atoms (29 $Å^2$). Therefore, it seems quite likely that the very mobile ϵ-amino group undergoes this small structural adjustment to carry out the catalysis.

Conformational Differences between αD60N and αD60N−IPP−Ser. The differences in structure between the αD60N mutant (*23*) and the starting model (the wild type structure in the presence of K^+) were measured. When the two molecules were compared on the basis of superposition of the "core" residues of the β-subunit as described previously (*13*), the rms deviation between all the main chain atoms in the α- and β-subunits was 0.52 Å. Relatively large deviations were only found near the mutation site, indicating that the mutation does not induce any significant global changes in structure.

The unliganded αD60N structure was then compared with the αD60N−IPP−Ser structure. After the corresponding core residues of the β-subunit were superimposed, the rms differences in position for each residue were calculated and shown in panels A and B of Figure 6 for the α- and β-subunits, respectively.

In the α-subunit of the αD60N−IPP−Ser structure, the binding of IPP results in localized small perturbations in loop 2 (residues 53−62) and in the IPP phosphate binding site (residues 212 and 213), and we note that αAsn60 in loop 2 is within 3.0 Å of the indolyl nitrogen of IPP. The loop 2 residues are mobile and have high temperature factors. The binding of L-serine to the β-subunit causes movement of as much as 2.6 Å of residues 93−189 of the β-subunit (Figure 6B).

DISCUSSION

Structural and Functional Roles of αAsp60. The α-subunit topology is an 8-fold α/β-barrel, originally observed in triosephosphate isomerase. αAsp60 is located in a region (residues 53−78) containing loop 2 (53−62) and helix 2′ (63−73) that is inserted into the canonical 8-fold α/β-barrel and is one of the most highly conserved regions of the α-subunit. Some residues in loop 2 are located in the interface between the α- and β-subunits and appear to be disordered or highly mobile. Mutagenesis studies (*17*, *27*) also suggest that αAsp60 could serve in a catalytic role.

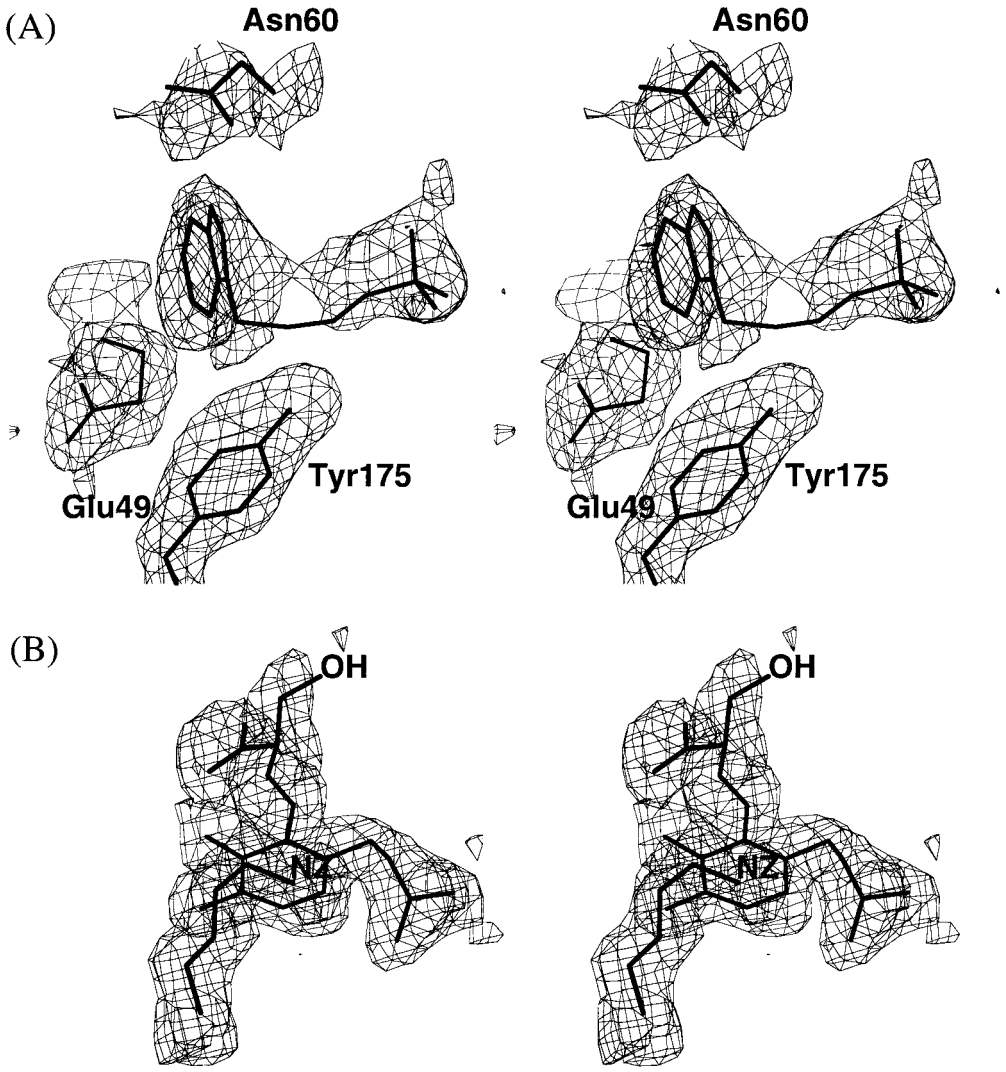

FIGURE 4: Final $2F_o - F_c$ map overlaid on the models of (A) IPP and residues αGlu49, αAsn60, and αTyr175 and (B) βLys87 and the external aldimines of the coenzyme pyridoxal 5′-phosphate with L-serine in the αD60N−IPP−Ser complex. The map was contoured at 0.6σ.

Spectroscopic and kinetic investigations of the effects of mutagenesis of αAsp60 in loop 2 (*5*) and of αArg179 in loop 6 (*6*) implicated these residues in the transmission of allosteric information between the active sites of the α- and β-subunits. Loop 6 (residues 178−191) is highly disordered and cannot be seen in the wild type structure (*1*). The spectroscopic and kinetic results suggested that binding of ligands to the active site of the α-subunit induces movements in loop 6 that convert the α-subunit from an "open" to a "closed" conformation. Modeling studies predicted that closure of loop 6 would place some of its residues in contact with residues in loop 2 (*6*). More detailed structural features have been obtained from the crystal structure of a mutant enzyme having ligands bound to both subunits (βK87T−IPP−Ser) (*13*). These results show clearly that α-subunit loops 2 and 6 become ordered and that the carboxylate side chain of αAsp60 interacts with both the indolyl nitrogen of IPP and the hydroxyl group of αThr183 in loop 6 (Figure 1). In addition, in the combined presence of both ligands, the β-subunit exhibits large conformational changes in a mobile subdomain (residues 93−189), and there is a rotation of the α-subunit relative to the β-subunit.

When both ligands are bound to the αD60N mutant (αD60N−IPP−Ser), the conformational changes in both subunits are much smaller than those observed in the βK87T−IPP−Ser structure. In striking contrast, α-subunit loop 2 remains mobile and loop 6 remains invisible, indicating that mutation of αAsp60 in loop 2 impairs the ability of the α-subunit to undergo a ligand-induced conformational change, probably by preventing the interaction of the carboxylate of αAsp60 with the indolyl nitrogen of IPP or the hydroxyl group of αThr183 in loop 6 or both. The failure of the mutant enzyme to undergo this ligand-induced change may prevent the transmission of allosteric information from the α-subunit to the β-subunit as discussed below. Studies of a related mutant (D60Y) $\alpha_2\beta_2$ complex suggested that altered kinetic behavior in the presence of an α-site ligand reflects an impaired ability of the mutant $\alpha_2\beta_2$ complex to undergo the conformational transition from the open to the closed form (*5*).

Effects of the αD60N Mutation on the Conformation of the β-Subunit. Allosteric interactions between the tryptophan synthase α- and β-subunits are very important for the function of the $\alpha_2\beta_2$ complex. Kinetic and spectroscopic

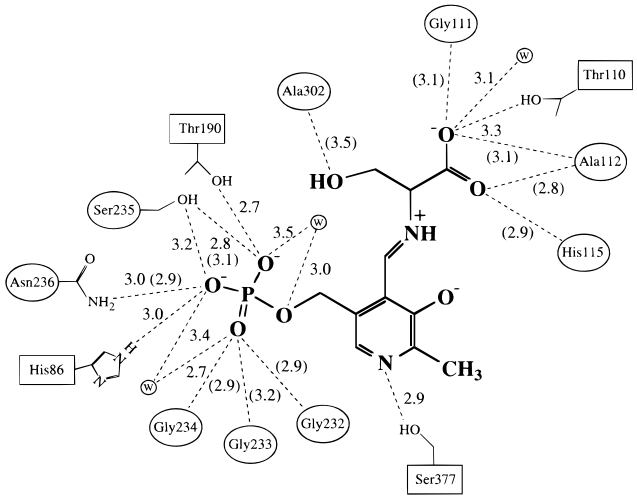

FIGURE 5: Interactions between polar atoms of the external aldimines and protein residues within 3.5 Å in the β-subunit of the αD60N−IPP−Ser complex. Residues are enclosed with an oval if their main chain atoms interact with polar atoms (oxygen or nitrogen) of the external aldimine or with a rectangle if their side chains alone contribute to polar interactions. If both the main chain and side chain atoms form interactions with the external aldimines, residues with the side chain are in an oval (see Ser235 and Asn236), and the corresponding interactions are indicated with dashed lines. The numbers correspond to interatomic distance in angstroms formed by the main chain atoms (in parentheses) or by the side chain atoms (without parentheses). Each water molecule is labeled within a small circle.

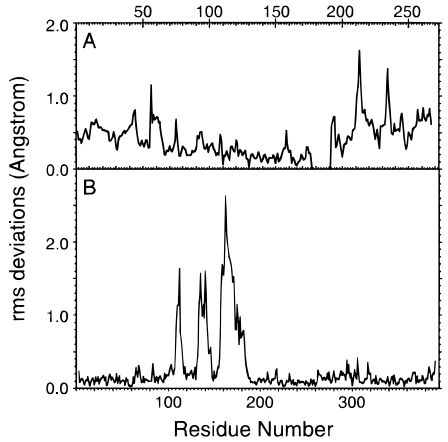

FIGURE 6: Plots showing the rms deviation in the main chain atoms for corresponding residues between αD60N (see ref *23*) and the αD60N−IPP−Ser complex after the core residues of the β-subunit are superimposed: (A) α-subunit and (B) β-subunit.

studies have shown that ligand binding to the active site of the α-subunit affects the equilibrium distribution of catalytic intermediates at the active site of the β-subunit (*3*). The primary intermediates in the reaction of L-serine are the aldimines between PLP and L-serine (E−Ser) and between PLP and the aminoacrylate (E−AA) (Scheme 1B). The equilibrium between these intermediates is modulated by pH, temperature, monovalent cation, and α-subunit ligands with the wild type $\alpha_2\beta_2$ complex as mentioned in Results (*25*, *26*). This equilibrium distribution of intermediates can also be modulated by mutations in either the α- or β-subunit. Studies of the reaction of a related mutant (αD60Y) $\alpha_2\beta_2$ complex with L-serine indicated that the same intermediates accumulate as in the reactions of the wild type enzyme (*5*). However, both the αD60N (Figures 2 and 3, inset) and the αD60Y enzymes display increased amounts of E−Ser and less E−AA.

Microspectrophotometric measurements of single crystals allow the characterization of the functional properties of a protein in the same physical state where the three-dimensional structure is determined (*28*). Therefore, a direct structure−function correlation can be obtained. These measurements can be useful for defining the optimal conditions for the selective accumulation of individual catalytic intermediates. For example, experimental conditions for the selective accumulation of the α-aminoacrylate (E−AA in Scheme 1; *24*, *25*) and the quinonoid species[2] (E-Q) have been determined in the crystals of the wild type $\alpha_2\beta_2$ complex.

These microspectrophotometric studies with the αD60N enzyme (Figures 2 and 3) show that accumulation of the E−Ser intermediate is very much favored in the crystal of αD60N. Factors that promote formation of E−AA by the wild type enzyme (e.g., low pH, GP, or Cs^+) have very little effect with the αD60N $\alpha_2\beta_2$ complex in the crystal. In contrast, decreasing the pH does result in a smaller increase in the formation of E−AA by the αD60N enzyme in solution in the presence of sodium with respect to that for the wild type (inset of Figure 2). Addition of Cs^+ to the αD60N enzyme results in a large increase in the formation of E−AA in solution (inset of Figure 3) but not in the crystal (Figure 3). Thus, crystallization of the αD60N $\alpha_2\beta_2$ complex affects the equilibrium distribution of intermediates in the reaction with L-serine and stabilizes the conformation of the enzyme that favors the external aldimine (E−Ser). This conformation has been proposed to be the open form of the enzyme, originally postulated on the basis of kinetic studies (*29*, *30*), analysis of the effects of mutation on reaction specificity and substrate-induced inactivation (*31*), and spectroscopic studies in solution (*25*, *26*, *32*).

Effects of the Crystal Lattice Contacts on the Conformational and Functional Properties of the Crystalline $\alpha_2\beta_2$ Complex. Generally, crystallization results in the selective stabilization of a single protein conformation among those conformations present in equilibrium in solution. Crystal lattice contacts play key roles in defining a particular conformation. Consequently, ligand-induced conformational changes that occur in the soluble enzyme may be hindered by lattice interactions in the crystal or may result in cracking of the crystal when the conformational changes are large enough to weaken the lattice contacts (reviewed in ref *28*).

A number of studies have shed light on the conformational and functional properties of the crystalline tryptophan synthase $\alpha_2\beta_2$ complex. Recent crystallographic studies with the ligand-soaked crystals have shown that the crystalline enzyme can form the E−AA intermediate that requires large ligand-mediated conformational changes (*33*). Earlier comparisons of the reaction rates of suspensions of microcrystals of the tryptophan synthase $\alpha_2\beta_2$ complex with those of the soluble enzyme demonstrated that the active sites of both the α- and β-subunits were active in both the soluble and crystalline enzymes but exhibited functional differences (*34*). Larger differences between the effects of ligands on the kinetic constants in the soluble and crystalline enzymes

[2] A. Mozzarelli, in preparation.

suggested that the transmission of ligand-induced conformational changes from one subunit to the other is reduced in the crystal due to crystal lattice forces. Microspectrophotometric studies on single crystals of the tryptophan synthase $\alpha_2\beta_2$ complex demonstrated that, although the crystalline and soluble enzymes form the same enzyme−substrate intermediates, in some cases the equilibrium distribution of these intermediates differs in the two states of the enzyme (*24*). Later work showed that the equilibrium distribution of the E−Ser and E−AA intermediates is shifted in favor of E−Ser in the crystal (*25*). The preferential stabilization of E−Ser in the wild type crystal also occurs in the αD60N $\alpha_2\beta_2$ complex studied here.

Comparison of the αD60N−IPP−Ser and βK87T−IPP−Ser Structures. Although L-serine is bound as the external aldimine in both the αD60N−IPP−Ser and the *β*K87T−IPP−Ser (*13*) crystal structures, the *β*-subunit exhibits much larger conformational changes (as much as 5 Å) in the *β*K87T−IPP−Ser crystal structure than in the αD60N−IPP−Ser structure. These changes include a rigid body rotation of part of the N-terminal domain (residues 93−189) relative to the rest of the *β*-subunit, which moves these two regions together and decreases the volume of the tunnel between the α- and *β*-subunits (*13*). These ligand-induced changes provide a structural basis for interpreting the allosteric properties of tryptophan synthase. The absence of these changes in the αD60N−IPP−Ser structure strongly suggests that the interaction of the carboxylate of αAsp60 with the indolyl nitrogen of IPP and the hydroxyl group of αThr183 in loop 6 is important for the transmission of allosteric information from the α-subunit to the *β*-subunit that results in conversion of the *β*-subunit from an open to a closed form.

REFERENCES

1. Hyde, C. C., Ahmed, S. A., Padlan, E. A., Miles, E. W., and Davies, D. R. (1988) *J. Biol. Chem. 263*, 17857−17871.
2. Miles, E. W. (1991) *Adv. Enzymol. Relat. Areas Mol. Biol. 64*, 93−172.
3. Miles, E. W. (1995) in *Subcellular Biochemistry, Volume 24: Proteins: Structure, Function, and Protein Engineering* (Biswas, B. B., and Roy, S., Eds.) pp 207−254, Plenum Press, New York.
4. Brzović, P. S., Ngo, K., and Dunn, M. F. (1992) *Biochemistry 31*, 3831−3839.
5. Brzović, P. S., Sawa, Y., Hyde, C. C., Miles, E. W., and Dunn, M. F. (1992) *J. Biol. Chem. 267*, 13028−13038.
6. Brzović, P. S., Hyde, C. C., Miles, E. W., and Dunn, M. F. (1993) *Biochemistry 32*, 10404−10413.
7. Dunn, M. F., Brzović, P. S., Leja, C., Pan, P., and Woehl, E. U. (1994) in *Biochemistry of Vitamin B6 and PQQ* (Marino, G., Sannia, G., and Bossa, F., Eds.) pp 119−124, Birkhauser Verlag, Basel, Switzerland.
8. Houben, K. F., and Dunn, M. F. (1990) *Biochemistry 29*, 2421−2429.
9. Kirschner, K., Lane, A. N., and Strasser, A. W. M. (1991) *Biochemistry 30*, 472−478.
10. Pan, P., and Dunn, M. F. (1996) *Biochemistry 35*, 5002−5013.
11. Ruvinov, S. B., Yang, X.-J., Parris, K., Banik, U., Ahmed, S. A., Miles, E. W., and Sackett, D. L. (1995) *J. Biol. Chem. 270*, 6357−6369.
12. Yang, L.-h., Ahmed, S. A., Rhee, S., and Miles, E. W. (1997) *J. Biol. Chem. 272*, 7859−7866.
13. Rhee, S., Parris, K. D., Hyde, C. C., Ahmed, S. A., Miles, E. W., and Davies, D. R. (1997) *Biochemistry 36*, 7664−7680.
14. Lim, W. K., Shin, H. J., Milton, D. L., and Hardman, J. K. (1991) *J. Bacteriol. 173*, 1886−1893.
15. Yang, X.-J., and Miles, E. W. (1993) *J. Biol. Chem. 268*, 22269−22272.
16. Rowlett, R., Yang L.-H., Ahmed, S. A., McPhie, P., Jhee, K.-H., and Miles, E. W. (1998) *Biochemistry 37*, 2961−2968.
17. Nagata, S., Hyde, C. C., and Miles, E. W. (1989) *J. Biol. Chem. 264*, 6288−6296.
18. Ahmed, S. A., Miles, E. W., and Davies, D. R. (1985) *J. Biol. Chem. 260*, 3716−3718.
19. Rhee, S., Parris, K., Ahmed, S. A., Miles, E. W., and Davies, D. R. (1996) *Biochemistry 35*, 4211−4221.
20. Otwinowski, Z. (1993) in *Data Collection and Processing* (Sawyer, L., Isaacs, N., and Bailey, S., Eds.) pp 56−62, Science and Engineering Research Council, Warrington, United Kingdom.
21. Brünger, A. T. (1992) *X-PLOR Version 3.1 A system for X-ray crystallography and NMR*, Yale University Press, New Haven, CT.
22. Jones, T. A., Zou, J. Y., Cowan, S. W., and Kjeldgaard, M. (1991) *Acta Crystallogr. A47*, 110−119.
23. Rhee, S., Miles, E. W., and Davies, D. R. (1998) *J. Biol. Chem. 273*, 8553−8555.
24. Mozzarelli, A., Peracchi, A., Rossi, G. L., Ahmed, S. A., and Miles, E. W. (1989) *J. Biol. Chem. 264*, 15774−15780.
25. Peracchi, A., Mozzarelli, A., and Rossi, G. L. (1995) *Biochemistry 34*, 9459−9465.
26. Peracchi, A., Bettati, S., Mozzarelli, A., Rossi, G. L., Miles, E. W., and Dunn, M. F. (1996) *Biochemistry 35*, 1872−1880.
27. Shirvanee, L., Horn, V., and Yanofsky, C. (1990) *J. Biol. Chem. 265*, 6624−6625.
28. Mozzarelli, A., and Rossi, G. L. (1996) *Annu. Rev. Biophys. Biomol. Struct. 25*, 343−365.
29. Anderson, K. S., Miles, E. W., and Johnson, K. A. (1991) *J. Biol. Chem. 266*, 8020−8033.
30. Dunn, M. F., Brzović, P. S., Leja, C., Houben, K., Roy, M., Aguilar, A., and Drewe, W. F., Jr. (1991) in *Enzymes dependent on pyridoxal phosphate and other carbonyl compounds as cofactors* (Fukui, T., Kagamiyama, H., Soda, K., and Wada, H., Eds.) pp 257−264, Pergamon.
31. Ahmed, S. A., Ruvinov, S. B., Kayastha, A. M., and Miles, E. W. (1991) *J. Biol. Chem. 266*, 21548−21557.
32. Strambini, G. B., Cioni, P., Peracchi, A., and Mozzarelli, A. (1992) *Biochemistry 31*, 7535−7542.
33. Schneider, T. R., Gerhardt, E., Lee, M., Liang, P.-H., Anderson, K. S., and Schlichting, I. (1998) *Biochemistry 37*, 5394−5406.
34. Ahmed, S. A., Hyde, C. C., Thomas, G., and Miles, E. W. (1987) *Biochemistry 26*, 5492−5498.

BI980779D